SYSTEMATIC ANALYSIS OF OCEAN COLOUR UNCERTAINTIES

Samantha Lavender [(1, 2)]

(1) *Pixalytics Ltd, 1 Davy Road, Tamar Science Park, Derriford, Plymouth, Devon, PL6 8BX, UK*
Email:slavender@pixalytics.com
(2) *School of Marine Science & Engineering, Plymouth University, Plymouth, Devon, PL6 8AA, UK*

ABSTRACT

This paper reviews current research into the estimation of uncertainties as a pixel-based measure to aid non-specialist users of remote sensing products. An example MERIS image, captured on the 28 March 2012, was processed with above-water atmospheric correction code. This was initially based on both the Antoine & Morel Standard Atmospheric Correction, with Bright Pixel correction component, and Doerffer Neural Network coastal water's approach. It's showed that analysis of the atmospheric by-products yield important information about the separation of the atmospheric and in-water signals, helping to sign-post possible uncertainties in the atmospheric correction results. Further analysis has concentrated on implementing a 'simplistic' atmospheric correction so that the impact of changing the input auxiliary data can be analysed; the influence of changing surface pressure is demonstrated. Future work will focus on automating the analysis, so that the methodology can be implemented within an operational system.

1. INTRODUCTION

Earth Observation products, such as maps of chlorophyll concentration and land vegetation, from future spaceborne missions will have continuity with existing / historical missions such as Envisat/MERIS and MODIS-Terra in terms of both the algorithms and products alongside the introduction of new approaches. Space agencies have also recognised the need for error and/or uncertainty estimates so that end users are provided with knowledge that allows them to have confidence in the data they're using.

Previous research, as part of the ESA Sentinel-3 Level-2 Optical Prototype Processor contract [4], primarily focused on the impact of the input data and algorithm / modelling uncertainties. Primarily, a sensitivity analysis approach was utilised; akin to the ensemble approach used by the modelling community.

The research within this paper is focused on investigating pixel based uncertainties for an example image as an expert user i.e. based on knowledge that has been gathered over a number of years. However, the longer-term ultimate aim is to develop methodologies and implement solutions that will allow uncertainty estimates to be calculated on a pixel-by-pixel basis whilst being efficiently processed for operational implementation.

2. APPLICATION TO ATMOSPHERIC CORRECTION

Eq. 1 is a simplification of the Atmospheric Correction (AC) equation where L_{toa} is the Top of Atmosphere (TOA) radiance (sensor radiance, which is measured), L_g is the ground radiance (term we are interested in deriving), T_d is the diffuse transmittance (reduction in the ground radiance by absorption within the atmosphere) and L_v is the veiling radiance (additional radiance scattered into the atmospheric path and reaching detector, through single and/or multiple scattering).

$$L_{toa} = L_g * T_d + L_v \qquad (1)$$

The Guide to the expression of Uncertainty in Measurement [5] states that "…when all of the known or suspected components of error have been evaluated and the appropriate corrections have been applied, there still remains an uncertainty about the correctness of the stated result, that is, a doubt about how well the result of the measurement represents the value of the quantity being measured." Therefore, uncertainty is a parameter that characterizes the dispersion of the values that could reasonably be attributed to the measurand. Also, a corrected measurement can unknowably be very close to the value of the measurand (i.e. have a negligible error), but at the same time may have a large uncertainty.

If we add uncertainties (τ) to Eq. 1 it becomes Eq. 2:

$$L_{toa} + \tau_{toa} = (L_g + \tau_g) * (T_d + \tau_d) + (L_v + \tau_v)$$
$$(2)$$

One approach to calculating standard uncertainty, which could result from random error (RE), is a Type A evaluation (Eq. 3) where s is the standard deviation and n is the number of measurements [5].

$$\text{standard uncertainty } (u) = \frac{s}{\sqrt{n}} \qquad (3)$$

When applied to remote sensing, as in Lavender et al. [4], the algorithm / model is run multiple times with variations in the input values (estimated uncertainties)

and the mean and standard deviation of the output is calculated. For the input values we are applying a Type B evaluation (Eq. 4) [5] where a is the mid-point between the upper and lower limits; only the limits of uncertainty are available until the previous step also has a Type A evaluation applied. The challenge is to expand outwards so that all the uncertainties for the inputs can be estimated, which quickly becomes a large effort.

$$\text{standard uncertainty } (u) = \frac{a}{\sqrt{3}} \qquad (4)$$

Therefore, for the simplified AC equation (Eq. 1), the combined standard uncertainty would then be calculated from Eq. 5 assuming the terms are uncorrelated. Where the inputs are significantly correlated, the covariance's need to also be estimated.

$$\frac{\tau_g}{L_g} = \sqrt{\left(\frac{2\tau_{toa}}{L_{toa}}\right)^2 + \left(\frac{\tau_v}{L_v}\right)^2 + \left(\frac{\tau_d}{2T_d}\right)^2} \qquad (5)$$

In addition, the usual assumption in data assimilation is that observational errors are unbiased; if biases are not effectively removed then the impact of the observation (i.e. satellite data) will be lessened and can even be detrimental. Therefore the bias, or total systematic error, would be calculated using Eq. 6; in practice it's related to the calculation of a mean or average.

$$\tau_g = \frac{\tau_{toa} - \tau_v}{\tau_d} \qquad (6)$$

For further information, in addition to [5], the National Physics Laboratory also has online tutorials on uncertainty http://www.npl.co.uk/publications/good-practice-online-modules/measurement-uncertainty/

The following Case Study focuses on an expert analysis of an example image in terms of understanding the spatial variability in the atmosphere versus ocean. Therefore, the results of visually analysing atmospheric by-products, veiling radiance (L_v) and diffuse transmittance (T_d), are reported as the first step. The second step is an analysis of the auxiliary data.

3. CASE STUDY: ANALYSIS OF AN EXAMPLE IMAGE

Fig. 1 is a MERIS Reduced Resolution (RR) image from the 28 March 2012. As seen in the TOA pseudo-true colour radiance image (Fig. 1a), there are areas of cloud cover to the North and South (bright white). Regions of high suspended sediment concentration can be seen around the United Kingdom (UK) as pixels with a yellow coloration: Irish Sea; Bristol Channel; English Channel;

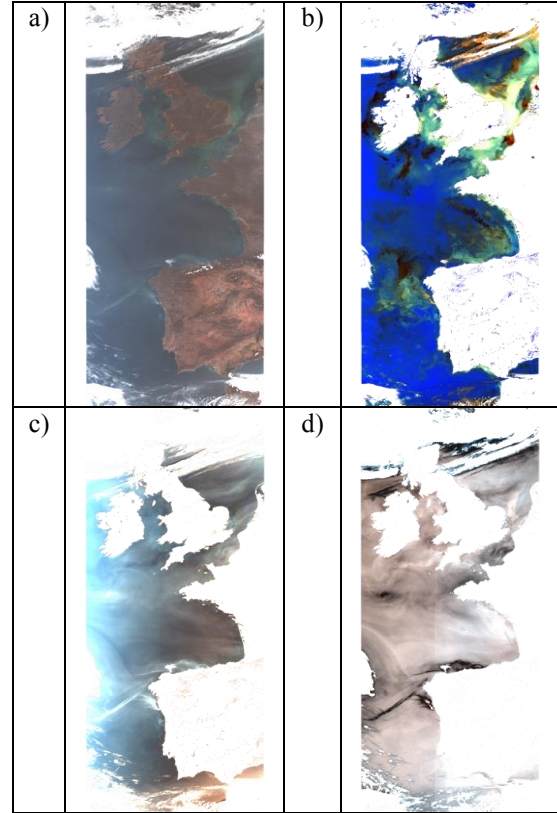Southern North Sea. Variations in chlorophyll are not readily visible.

Figure 1. 28 March 2012 Envisat MERIS Image as Pseudo-True Colour (bands 7, 4 & 2) images for a) Top of Atmosphere Radiance, b) Bottom of Atmosphere Radiance, c) Path Radiance and d) Diffuse Transmittance.

The Bottom of Atmosphere (BOA) radiance image (Fig. 1b) derived using the Case2R Neural Network (NNet), run within BEAM VISAT (http://www.brockmann-consult.de/cms/web/beam/), and displays an output that enhances the prominence of the in-water features. The sediment concentration variation is much more visible alongside the variations in chlorophyll within the Bay of Biscay and off the coast of Portugal.

Fig. 1c and Fig. 1d are images of the atmosphere components; path radiance and diffuse transmittance respectively. As the atmosphere typically has larger spatial scales than the ocean, sharp features wouldn't be expected within these two atmospheric products unless there are point sources such as fires. For the NNet approach it should be noted that the atmospheric products are not subtracted from the sensor radiance during the processing, but rather the elements are decomposed and then the atmospheric by-products calculated.

To investigate further, the Level 1 RR MERIS image was also processed using ODESA

(http://earth.eo.esa.int/odesa/) with the 3rd MERIS reprocessing settings. Fig. 2 shows the diffuse transmission from the Antoine & Morel [1] Standard AC (SAC), including the Moore & Lavender [2] Bright Pixel AC (BPAC), and the Doerffer [3] Case 2 NNet. The SAC shows a much smoother pattern of transmission variation off the East coast of the UK in the southern North Sea, indicating that the feature seen in the Case2 NNet (southern North Sea) output is a water rather than atmospheric signal; has a pattern reminiscent of the sediment distributions seen in Fig. 1a.
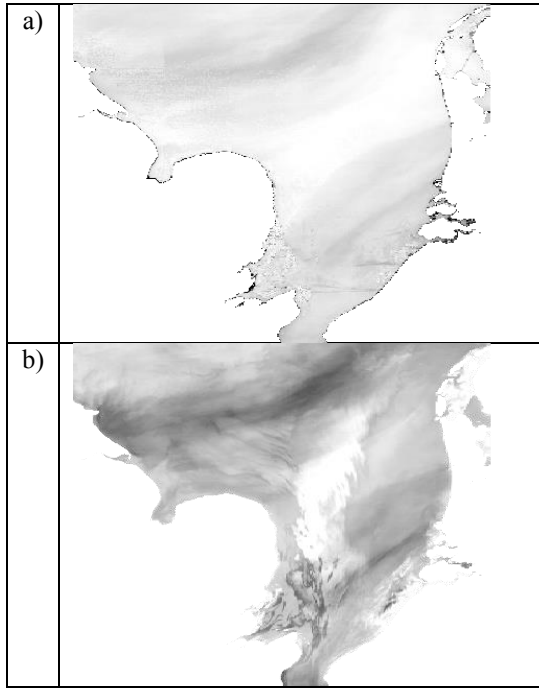

Figure 2. 28 March 2012 Envisat MERIS Image processed in ODESA with the a) Standard Atmospheric Correction and b) Case 2 Neural Network; atmospheric diffuse transmission being displayed.

To investigate further the 'Goodness of Fit' for both the AC and In-Water NNets was examined (Fig. 3), which provides an insight into how well the trained NNet is able to model the provided radiance spectra; available when processing data through ODESA, but not currently available in the standard output product due to the Envisat N1 size / format restrictions. Another important source of information (not shown) is the indication of 'out of scope' which highlights where the model has received real data that is considered within scope of the training dataset / methodology used e.g. concentration ranges.

Eq. 7 is the calculation of chi_sum [3] where 12 is the number of bands being used within the NNet, RL_{tosa} is the measured input NNet spectra and outnet is the spectra from the auto-associative NNet that tests if the measured spectra can be reproduced:

$$\text{chi\_sum} = \sqrt{\frac{\sum_{0}^{i<12}\left(\frac{\log(RL_{tosa}[i]) - \text{outnet}[i]}{\log(RL_{tosa}[i])}\right)^2}{12}}$$

(7)

The chi_sum output for the AC NNet (Fig. 3a) highlights the spatial variability of the NNet solution when separating the atmospheric and in-water signals, with a larger chi_sum value for the turbid water pixels.
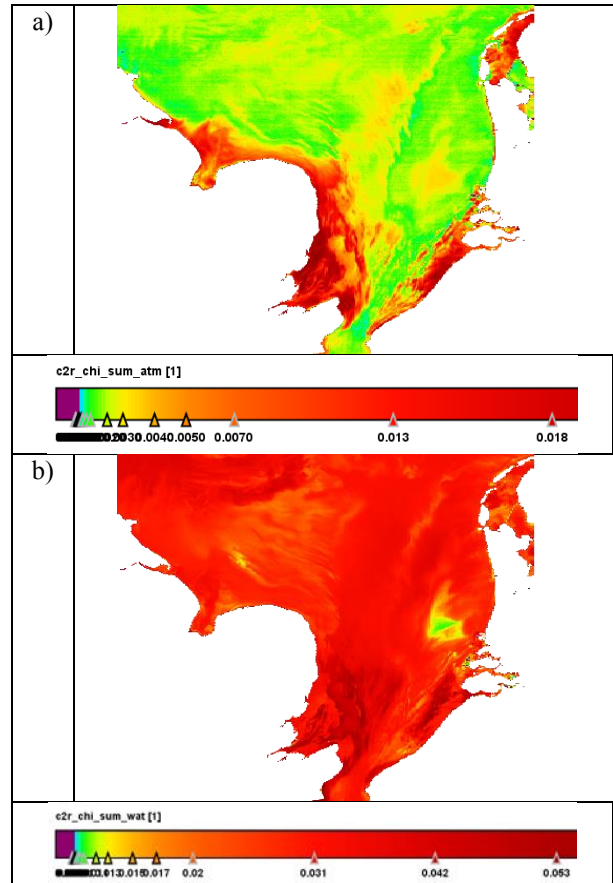

Figure 3. 28 March 2012 Envisat MERIS Neural Network Goodness of Fit for the a) Atmospheric Correction and b) In-Water Neural Networks.

To understand the input uncertainties caused by the auxiliary data, focusing on the meteorological data initially, a 'simplistic' AC [6] was updated to process MERIS imagery; single scattering aerosol estimation using the angstrom exponent for aerosol extrapolation i.e. a 'CZCS type' approach. For initial tests the BPAC has also been switched off (so there is no iteration / non-linearity) and no flagging/masking of pixels is included.

Fig. 4a displays the Bottom of Atmosphere Reflectance processed and a plot (for a single pixel) of the change in Bottom of Atmosphere Reflectance caused by adjusting

the atmospheric pressure; European Centre for Medium-term Weather Forecast (ECMWF) mean sea level pressure values are included within the Level 1b data on an interpolated tie-point grid; as the data is reprocessed then ECMWF analysis data is used.
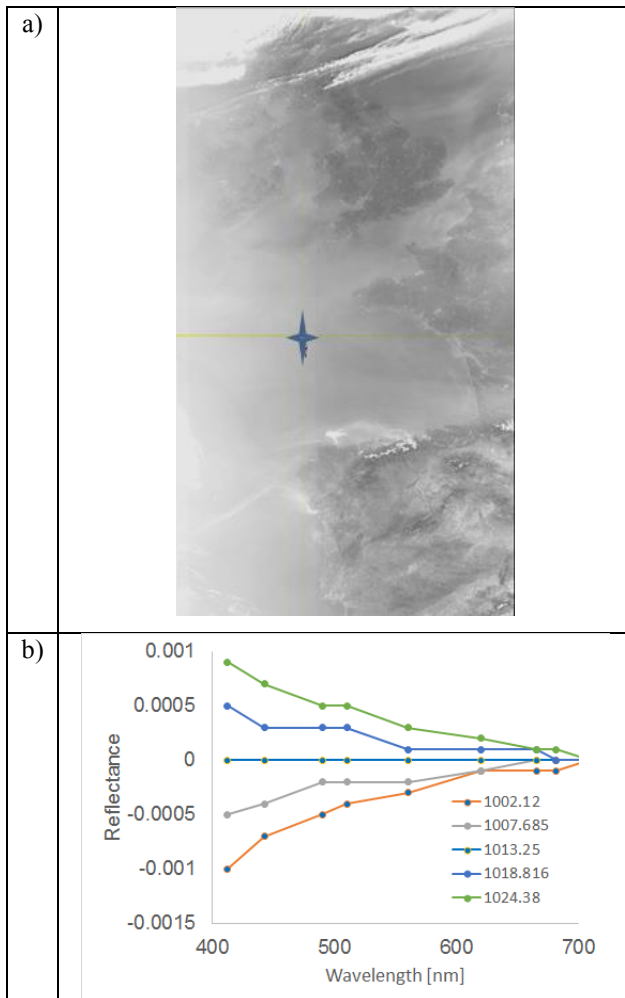

Figure 4. 28 March 2012 Envisat MERIS Image as (a) Pseudo-True Colour (bands 7, 4 & 2) Bottom of Atmosphere Reflectance processed using a simplistic atmospheric correction and (b) Plot of change in Bottom of Atmosphere Reflectance caused by adjusting the atmospheric pressure. The yellow lines/blue star mark the position of the extracted pixel shown in plot (b).

The currently processed image probably indicates that an insufficient atmospheric signal has been subtracted as the BOA is still very hazy. However, this does not invalidate the results shown for atmospheric pressure. The image was processed with the standard atmospheric pressure (1013.25 hPa) whereas the MERIS auxiliary data suggests the value should be higher (over the whole image; mean of 1027.02 hPa, minimum of 1014.43 hPa and maximum of 1033.83 hPa). However, the error caused by using the wrong value will be small; BOA

reflectance change of less than 0.001 at the shortest wavelength for the atmospheric pressure range used. The differences are higher in the blue as the atmospheric pressure influences the determination of the Rayleigh scattering.

4. DISCUSSION AND CONCLUSIONS

This paper reviewed the approach to calculating uncertainties numerically, but in the case study the expert analysis is visual as the research is at a preliminary stage. A second step is shown where the input data is variability and the sensitivity of the output analysed.

The next step is to understand the outputs further by running the analysis on a number of images and ultimately determine a technique that will provide an automatic uncertainty flagging / analysis system.

In Summary:
- There are several methods to look at uncertainty:
  - Propagation of uncertainty through equations i.e. sensitivity of the output to the input (akin to the ensemble approach used within the modeling community);
  - "Goodness of fit" indicating how well the model understands the inputs.

- Running a simplistic model in parallel with more complex approaches can be used to understand what the complexity is contributing

- As an "expert" we use our eyes/brain to look for inconsistencies in products. Can we automatically capture this process?

- In the end, the "non-expert end user" wants a probability that the answer can be believed…. Should be simple to understand even if getting there is complex.

5. REFERENCES

1. Antoine, D. and Morel, A. 2011. Atmospheric Correction of the MERIS observations Over Ocean Case 1 waters. *MERIS ATBD 2.7*, Iss. 5 Rev. 1 **http://envisat.esa.int/instruments/meris/atbd/atbd_2.7.pdf**
2. Moore, G. and Lavender, S. 2011. Algorithm Identification: Case II.S Bright Pixel Atmospheric Correction. MERIS ATBD 2.6, Iss. 5.0 **http://envisat.esa.int/instruments/meris/atbd/atbd_2.6.pdf**

3. Doerffer, R. 2011. Alternative Atmospheric Correction Procedure for Case 2 Water Remote Sensing using MERIS. *MERIS ATBD 2.25*, v1.0 **http://envisat.esa.int/instruments/meris/atbd/abtd_2.25_v1.0.pdf**

4. Lavender, S., Fanton d'Andon, O., Kay, S., Bourg, L., Emsley, S., Gilles, N., Nightingale, T., Quast, R., Bates, M., Storm, T., Hedley, J., Knul, M., Sotis, G., Nasir-Habeeb, R., Goryl, P. and Sentinel-3 L2 Products and Algorithm Team. 2012. Applying Uncertainties to Ocean Colour Data. Metrologia, 49, S17, doi:10.1088/0026-1394/49/2/S17

5. JCGM. 2008. Evaluation of measurement data – Guide to the expression of uncertainty in measurement (GUM) **http://www.bipm.org/utils/common/documents/jcgm/JCGM_100_2008_E.pdf**

6. Lavender, S.J. and C.R.C. Nagur. 2002. Mapping coastal waters with high resolution imagery: atmospheric correction of multi-height airborne imagery, J. Opt. A: Pure Appl. Opt., 4, S1–S.

6. ACKNOWLEDGEMENTS